Biophysical Journal, Volume *115*

Supplemental Information

Computational Model of Chimeric Antigen Receptors Explains Site-Specific Phosphorylation Kinetics

Jennifer A. Rohrs, Dongqing Zheng, Nicholas A. Graham, Pin Wang, and Stacey D. Finley

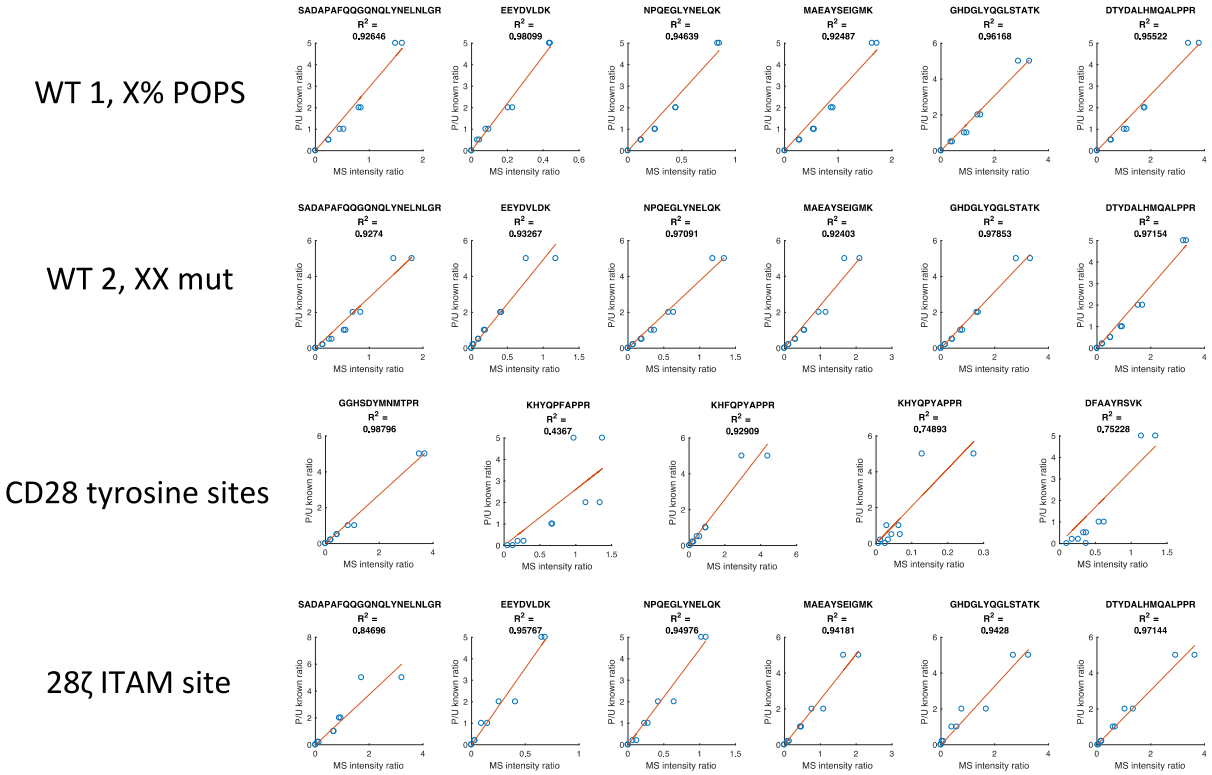

Figure S1: Standard curves for phosphorylated:unphosphorylated peptide intensity normalization. Data was collected on the mass spectrometer in three sets, and each set was normalized by a standard curve collected at the same time. All of the standard curves used are shown here, with each row being used to analyze a separate set of data. Row 1 was used to analyze the first biological replicate of the wild type ITAM phosphorylation on 10% POPS liposomes and the wild type ITAM phosphorylation on 0% and 45% POPS liposomes. Row 2 was used to analyze the second biological replicate of the wild type ITAM phosphorylation on 10% POPS liposomes as well as the individual tyrosine to phenylalanine CD3ζ ITAM point mutants. The third and fourth rows were used to analyze all 28ζ proteins, including the Y206F and Y209F mutants.

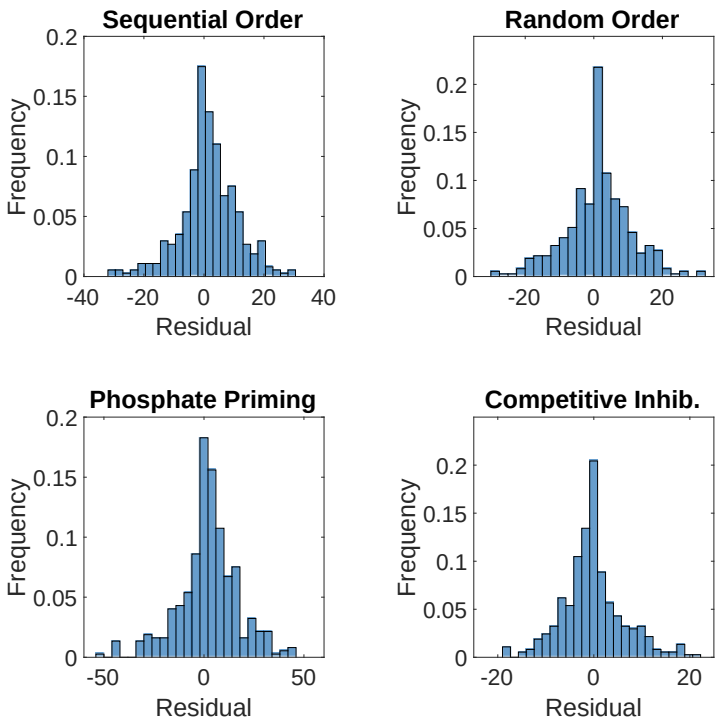

Figure S2: Histogram of residual distributions for the best fit parameter sets. Each mechanistic model was fit to the data, as described in the methods. The best fit parameter set for each model was then used to calculate the residuals between the model predictions and the experimental data for all timepoints and all experimental conditions of CD3ζ and its tyrosine to phenylalanine mutants. The histograms show the distribution of the residuals for each individual model.

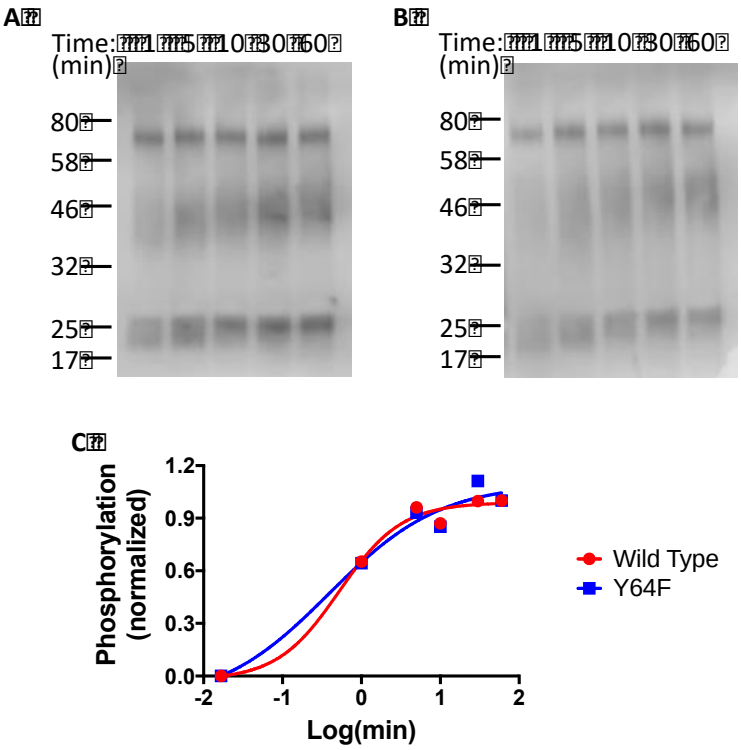

Figure S3: Comparison of wild type and Y64F CD3ζ phosphorylation rates. (A, B) Western blot of CD3ζ phosphorylation time courses. Liposomes bearing ~10,000 molecules/μm^2 of wild type CD3ζ (A) or CD3ζ-Y64F (B) and ~155 molecules/μm^2 of LCK-Y505F were allowed to react in the presence of ATP, as described in the Methods. At various times, the reaction was stopped by adding one volume of 10x SDS PAGE running buffer (Millipore Sigma) and boiling for 5 minutes. Samples were then analyzed by western blotting with anti-phospho-tyrosine antibodies. Blots were analyzed using the C-DiGit Western Blot Scanner (Li-Cor Biosciences – U.S.). (C) Quantification of CD3ζ phospho-tyrosine western blots. The intensity of the CD3ζ monomer bands (~23 kDa) was analyzed using the Image Studio Digits Software (Li-Cor Biosciences – U.S., version 3.1). Signal intensities for each protein (wild type and Y64F mutant) were normalized by the signal at 60 minutes and a standard sigmoidal curve was fit to the data.

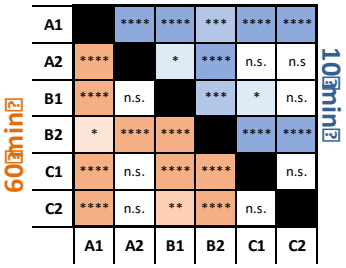

Figure S4: Statistical comparison of CD3ζ ITAM site phosphorylation levels. (Blue) 10 minute comparison, (Orange) 60 minute comparison. Measured by pairwise Tukey t-tests (**** $p<0.0001$, *** $p<0.001$, ** $p<0.01$, * $p<0.05$, n.s. not significant).

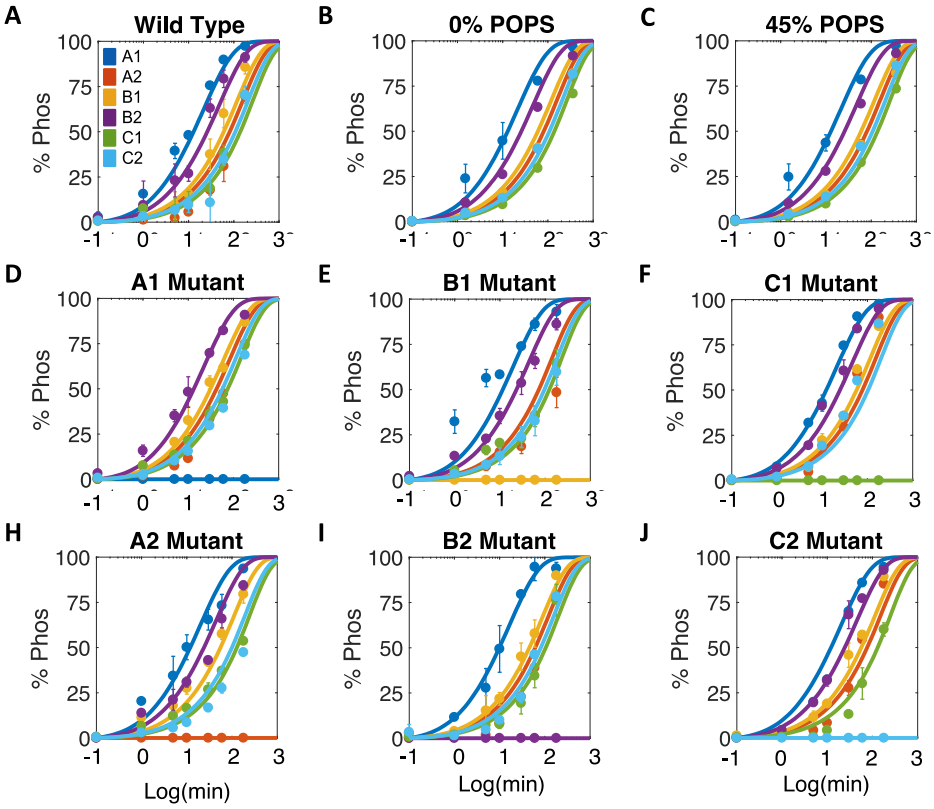

Figure S5: CD3ζ ITAM site phosphorylation model fits. (A) The second biological replicate of wild type CD3ζ ITAM protein stimulated on liposomes containing 10% POPS lipids, (B) wild type CD3ζ ITAM protein stimulated on liposomes containing 0% POPS lipids, (C) wild type CD3ζ ITAM protein stimulated on liposomes containing 45% POPS lipids. (D-J) CD3ζ proteins bearing individual tyrosine to phenylalanine ITAM point mutations stimulated on liposomes containing 10% POPS lipids.

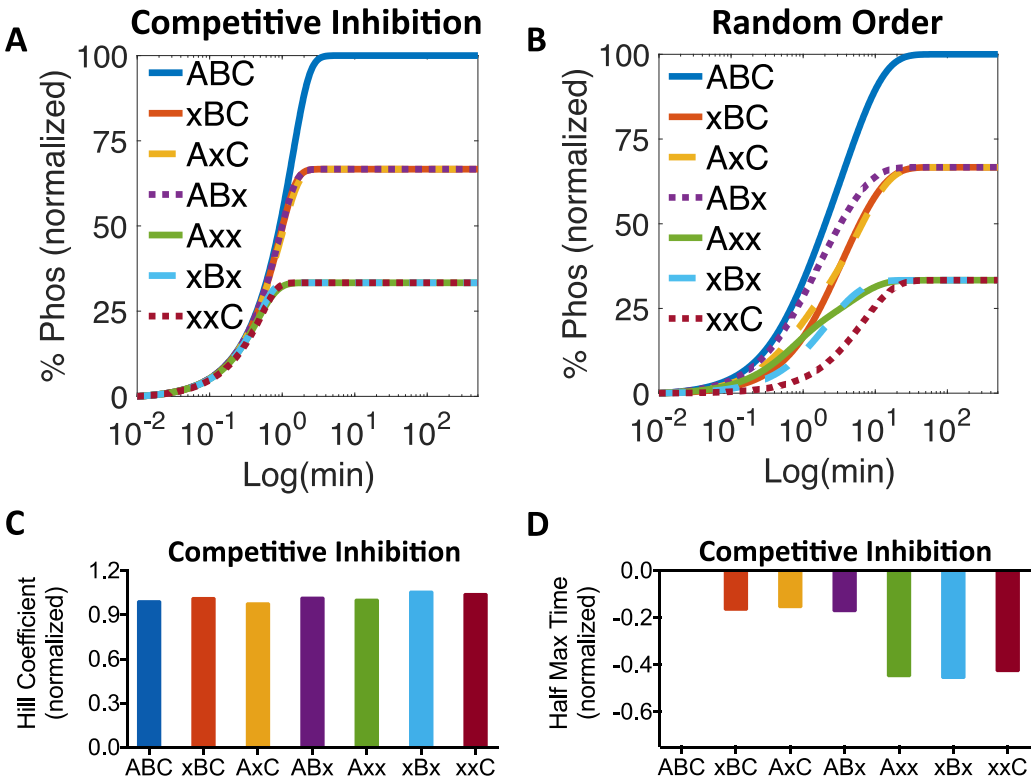

Figure S6: Model predictions for ITAM mutant phosphorylation profiles.

(A) Predicted phosphorylation profiles for wild type, single, and double ITAM mutant CD3ζ with the competitive inhibition model. Mutated ITAMs are indicated by (x). Model was implemented using the optimal parameters from the model fitting shown in **Figure 3D** with initial conditions of 20 LCK/μm^2 and 2000 CD3z/μm^2.

(B) Predicted phosphorylation profiles for wild type, single, and double ITAM mutant CD3ζ with the random order model. Mutated ITAMs are indicated by (x). Model was implemented using the optimal parameters from the model fitting shown in **Figure 3B** with initial conditions of 20 LCK/μm^2 and 2000 CD3z/μm^2.

(C) Hill coefficient of the phosphorylation response predicted by the model for each CD3ζ mutant in the competitive inhibition model.

(D) Half maximal time of the predicted phosphorylation response for each CD3ζ mutant in the competitive inhibition model.

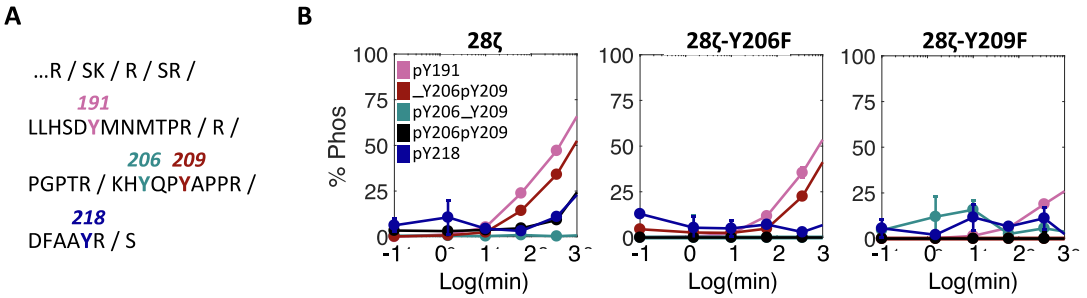

Figure S7: CD28 phosphorylation profiles.

(A) Sequence of CD28 intracellular domain with trypsin cut sites denoted. Individual tyrosine sites are labeled in different colors.

(B) Experimental data for CD28 tyrosine site phosphorylation on wild type CD28-CD3ζ, CD28-Y206F-CD3ζ, and CD28-Y209F-CD3ζ. Error bars represent the standard deviation of two technical replicates normalized by site-specific standard curves.